Lifetime-separated spectroscopy: Observation and rotational analysis of the BaO $A'\,^1\Pi$ state

J. Gary Pruett and Richard N. Zare

Department of Chemistry, Columbia University, New York, New York 10027
(Received 7 November 1974)

The BaO $A'\,^1\Pi$–$X\,^1\Sigma^+$ band system has been investigated using laser-induced fluorescence. The BaO is formed in the gas-phase reaction Ba + CO_2 under single-collision conditions, and the $A'\,^1\Pi$ and $A\,^1\Sigma^+$ states are simultaneously excited by a pulsed tunable dye laser with a 0.2 Å bandwidth. The weak, long-lifetime A'–X fluorescence is separated from the strong, short-lifetime A–X fluorescence by delaying the observation of the A'–X emission until the A–X emission dies away. The lifetime of the BaO $A'\,^1\Pi$ state is found to be 9 ± 1 μsec, more than an order of magnitude longer than that of the BaO $A\,^1\Sigma^+$ state. We have observed the $(v',0)$ band progression for $9 \leq v' \leq 18$ as well as the (10,1) and (13,1) bands of the A'–X system, and they are found to be represented by the A' state vibrational constants $\nu_{00} = 17\,573 \pm 10$ cm^{-1}, $\omega_0 = 442.38 \pm 1.1$ cm^{-1} and $\omega_0 x_0 = 1.693 \pm 0.025$ cm^{-1}. The (12,0), (17,0), and (18,0) bands have been rotationally analyzed, yielding the rotational constants $B_{12} = 0.20849 \pm 0.00022$ cm^{-1}, $B_{17} = 0.20290 \pm 0.00012$ cm^{-1}, and $B_{18} = 0.20109 \pm 0.00014$ cm^{-1}. These results confirm that the shapes of the potential curves for the $A'\,^1\Pi$ and $a\,^3\Pi$ states of BaO are remarkably similar for low vibrational levels. We also conclude that the $A'\,^1\Pi$ state is not the emitter responsible for the many-line emission spectrum seen in the Ba + N_2O and Ba + O_3 reactions at low pressures, nor is it the "dark" precursor responsible for the high photon yields observed in these chemiluminescent reactions at high pressures.

I. INTRODUCTION

A general problem confronting those who analyze molecular spectra is the location of weak electronic transitions overlapped by strong electronic transitions. In either absorption or emission studies the stronger band system may obscure the weaker band system to such an extent that the presence of the latter often goes undetected. The stronger band system derives its intensity from its larger oscillator strength which, in turn, is usually associated with a shorter radiative lifetime. This suggests that the stronger and weaker bands can be separated from one another by observing the time decay of the molecular emission following pulsed excitation by light or other suitable means.

This may be put on a quantitative basis by letting τ_s and τ_w denote the radiative lifetimes of the strong and weak bands and letting I_s and I_w denote their initial emission intensities following the excitation pulse. Normally $I_s \gg I_w$ as well as $\tau_s^{-1} \gg \tau_w^{-1}$. The total intensity of the molecular emission $I(t)$ as a function of time is given by

$$I(t) = I_s \exp(-t/\tau_s) + I_w \exp(-t/\tau_w) \quad , \tag{1}$$

where we assume for simplicity that the decay of one state does not populate the other. Equation (1) is just the sum of the strong band and weak band emission intensities. Because the emission from the strong band system decays so much more rapidly than that from the weak band system, it is possible to detect the weak band emission by delaying the observation of the molecular emission for a time t equal to several multiples of the strong band lifetime, i.e., $t = n\tau_s$. After this time duration, Eq. (1) shows that the strong band emission has been reduced by $\exp(-n)$ of its initial value while the weak band emission has only been decreased by $\exp(-n\tau_s/\tau_w)$ of its initial value. For $\tau_s \ll \tau_w$, $n\tau_s/\tau_w$ may be less than unity. Under these favorable conditions, the strong and weak emissions can be almost completely separated from one another by virtue of their different lifetimes without significant reduction in the total emission signal from the weak band system.

Over one hundred years ago, Becquerel first exploited this principle to separate fluorescence from phosphorescence by using a simple mechanical shutter device involving rotating slotted discs (phosphoroscope) to interrupt the excitation source.[1] Since then, there has been widespread application of this technique to the study of luminescence from condensed media, but not from gases.[2] We report here the use of time delayed observation of pulsed luminescence in gaseous BaO to separate the overlapping fluorescence from two excited singlet states.[3] Unlike condensed media, the BaO experiments can be carried out at such low pressures that the excited states of BaO experience no collisions, on the average, before radiating. Consequently, the short lifetime state does not "feed" the long-lifetime state, and the fluorescence spectra of both states are collisionally undegraded. Thus it is possible to determine the structure of the isolated molecular state from an analysis of its lifetime-separated emission spectrum.

The excited electronic states of BaO are of considerable interest, because recent work on the nature of Ba + oxidant chemiluminescent flames suggests that these reactions are promising for the development of a visible chemical laser, based on the observed high quantum yields and the specificity of the emitting BaO states.[4–7] In order to develop kinetic schemes capable of modeling the observed chemiluminescent behavior, knowledge of the lifetimes and term values of the excited electronic states of BaO is necessary.

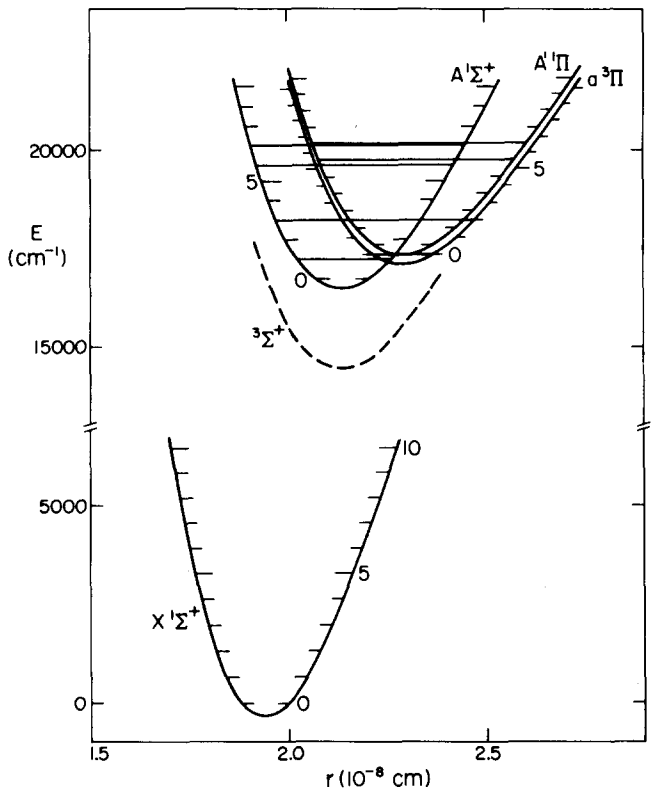

FIG. 1. Potential energy curves for BaO, taken from the work of Field, Jones, and Broida,[5] and reproduced with their permission. Vibrational levels are marked on all but the $^3\Sigma^+$ curve (dashed line) which is assumed to have the same shape as the $A\ ^1\Sigma^+$ curve, lowered by 2000 cm^{-1}. The strongest perturbations of the $A\ ^1\Sigma^+$ state are indicated by horizontal lines connecting the turning points of the perturbed levels.

Figure 1, taken from the work of Field, Jones, and Broida,[5] shows the four known electronic states of BaO. There is also believed to be a $^3\Sigma^+$ electronic state located between the X and A states.[8] The BaO X state has been well characterized by molecular beam electric resonance experiments.[9] In addition, information has been provided about the X state as well as the A state from the spectroscopic analysis of the BaO $A\ ^1\Sigma^+$–$X\ ^1\Sigma^+$ blue–green band system.[10–12] Rotational information on the A state has also been obtained by microwave optical double resonance experiments.[13] In the course of the observations of the optical spectra, Lagerqvist, Lind, and Barrow noted numerous perturbations in the A state which they suggested are caused by interaction with a neighboring $^1\Pi$ and $^3\Pi$ state. Using only the data of Lagerqvist and co-workers, Field[8] has assigned the perturbations of the $A\ ^1\Sigma^+$ state to a $^1\Pi$ state, denoted as $A'\ ^1\Pi$, and to three components of an inverted $^3\Pi$ state, denoted as $a\ ^3\Pi$. His analysis yielded vibrational and rotational constants for both perturbing states, under the assumption that the rotational and vibrational constants for the A' state are the same as for the a state. Although the $a\ ^3\Pi$ state has not been directly observed, weak $A'\ ^1\Pi$–$X\ ^1\Sigma^+$ emission in a flame of Ba burning at low pressure in the oxidants N_2O, NO_2, and O_2 has recently been photographed by Hsu, Krugh, Palmer, Obenauf, and Aten.[14] They observed a long $(v', 0)$ progression overlapped by a short $(v', 1)$ progression in the violet and ultraviolet. They identified the emitter as the BaO $A'\ ^1\Pi$ state by the excellent fit of the band head positions to Field's vibrational constants. They were unable to follow these progressions to longer wavelengths because of the strong interference from the A–X emission in the blue–green. Their resolution did not permit a rotational analysis of the observed bands.

The relative weakness of the BaO A'–X band system compared to the A–X band system can be rationalized on the basis of simple molecular orbital arguments.[15] The BaO molecule may be regarded as an eight valence electron system. The BaO $X\ ^1\Sigma^+$ ground state ($Ba^{++}O^{--}$) arises from the configuration (O; $2s\sigma)^2$ (O; $2p\sigma)^2$ (O; $2p\pi)^4$, the BaO $A\ ^1\Sigma^+$ state from the configuration (Ba; $6s\sigma$) (O; $2s\sigma)^2$ (O; $2p\sigma$) (O; $2p\pi)^4$, while the BaO $A'\ ^1\Pi$ and $a\ ^3\Pi$ states from the configuration (Ba; $6s\sigma$) (O; $2s\sigma)^2$ (O; $2p\sigma)^2$ (O; $2p\pi)^3$. The strength of the parallel Σ–Σ transition is proportional to the square of the dipole transition matrix element $\langle$(Ba; $6s\sigma$)$|z|$(O; $2p\sigma$)$\rangle$ and that of the perpendicular Π–Σ transition to $\langle$(Ba; $6s\sigma|x$ or $y|$(O; $2p\pi$)$\rangle$. For the A–X band system the dipole transition moment should be large because the (Ba; $6s\sigma$) and (O; $2p\sigma$) orbitals should overlap, corresponding to a strong charge transfer band; for the A'–X band system, the dipole transition moment should be small because it vanishes to the extent that the (Ba; $6s\sigma$) and the (O; $2p\pi$) orbitals are nonoverlapping. Consequently, the radiative lifetime of the BaO $A\ ^1\Sigma^+$ state is expected to be much shorter than the BaO $A'\ ^1\Pi$ state.

Indeed, confirmation of the existence of two BaO electronic states with substantially different lifetimes has been provided previously in the fluorescence decay studies by Johnson[16] who used a short-pulsed (10 nsec) tunable dye laser as an excitation source. He found in addition to the rapid decay of the A–X emission ($\tau = 356 \pm 7$ nsec for $v' = 0$), a second fluorescence decay with a lifetime of 10 ± 2 μsec at higher pressures, which he attributed to collisional transfer from the A state to a more long-lived, but unidentified state.

We report here the study of the $A'\ ^1\Pi$–$X\ ^1\Sigma^+$ bands free of the $A\ ^1\Sigma^+$–$X\ ^1\Sigma^+$ bands using lifetime-separated spectroscopy, as described above. This has allowed both lifetime measurements and a rotational analysis of the $A'\ ^1\Pi$ state. A discussion of the implications of these results to the Ba + oxidant chemiluminescent flame studies is also presented.

II. EXPERIMENTAL

The BaO molecules are formed from the gas-phase reaction $Ba + CO_2 \rightarrow BaO + CO$ in a molecular beam scattering apparatus, which has been described elsewhere.[17] Because this reaction produces BaO predominantly in the $X\ ^1\Sigma^+$ $(v = 0)$ level, it is ideally suited to provide absorbing molecules for the $(v', 0)$ progression seen by Palmer's group. In this apparatus (see Fig. 2) we use a "beam + gas" arrangement in which a beam of barium atoms from an oven at 1100 °K traverses a scattering chamber filled with CO_2 at a pressure of typically 5×10^{-4} torr and a temperature of 300 °K. The BaO formed along the path of the Ba beam is detected by the laser fluorescence technique.[18] A pulsed nitrogen-laser-

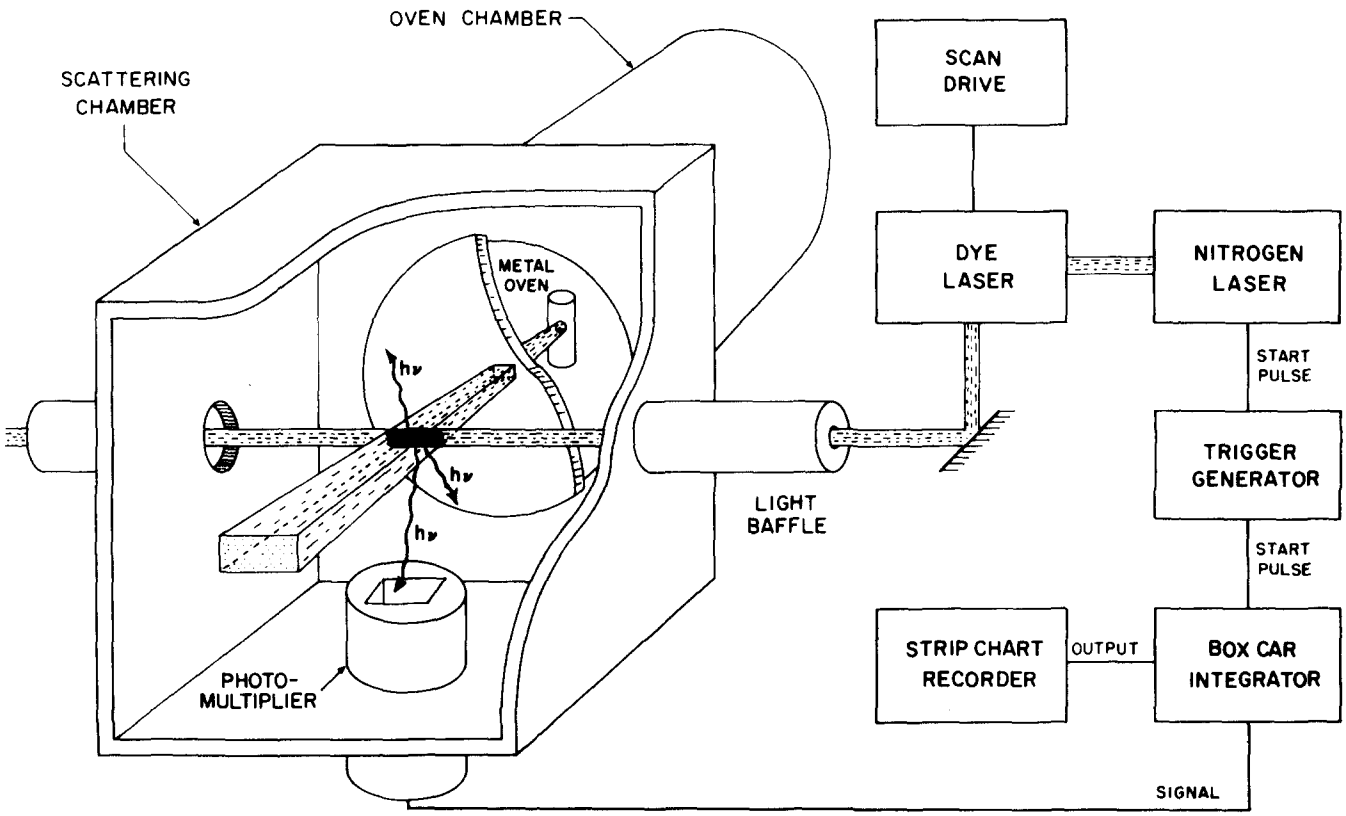

FIG. 2. Experimental setup: Perspective of the "beam + gas" scattering apparatus and schematic of the laser fluorescence detection system.

pumped tunable dye laser with 0.2 Å bandwidth, 10 nsec duration, and operating at 20 pps is directed through the beam-gas intersection region and is tuned from 4000 to 4750 Å using several dyes (see Table I). A photomultiplier tube (RCA 7265, S-20 photocathode, 2300 V) collects approximately 10% of the resulting molecular fluorescence. The output signal of the photomultiplier provides the input to a PAR model 162 boxcar integrator with a model 164 plug-in. A pulse from the nitrogen laser trigger generator, which is synchronous with the firing of the nitrogen laser (Molectron UV-300), triggers the boxcar averager. By suitably adjusting the boxcar gate delay and gate width, it is possible to obtain the time decay of the fluorescence or to separate the $A'-X$ fluorescence from the $A-X$ fluorescence.

For lifetime studies the gate width must be chosen to be a small fraction of the lifetime of the state under investigation. Since two lifetimes were involved, we chose a gate width of 200 nsec to assure resolution of the longer lifetime. The gate delay is automatically scanned by the boxcar from -1.0 to 50 μsec relative to the dye laser pulse. The scan rate is set at 50 nsec per second which allows averaging of 80 laser shots in each 200 nsec interval. The boxcar output drives a stripchart recorder running at 1.0 in./min, resulting in a fluorescence plot with a time scale of 3 μsec/in. Boxcar time base accuracy and stripchart timebase accuracy were calibrated to 0.5% using a crystal controlled frequency counter, giving a decay plot accuracy of better than 1%.

For spectroscopic studies of the $A'-X$ band system, the gate delay is fixed at 2 μsec, and the gate width is set to 20 μsec (approximately two A' state lifetimes). This results in an essentially complete separation of the $A-X$ and $A'-X$ fluorescence, regardless of the strength of the $A-X$ emission. We are, however, limited in our separation attempts by saturation of the photomultiplier. In several regions of the spectrum, extremely strong $A-X$ fluorescence overloads the photomultiplier, which is unable to recover before the boxcar gate is opened. This results in a negative baseline excursion, masking the desired $A'-X$ fluorescence signal. This limitation could be overcome, for example, by applying dynode gating techniques to "blind" the phototube to the strong short lifetime signal.

For measurement of $A'-X$ band head positions, the wavelength of the dye laser output is calibrated by measuring the wavelength at the peak of the dye laser gain using a 1 m Interactive Technology monochromator. Separate calibration of the monochromator using standard lines from a Hg lamp reveals a nominal error of

TABLE I. Organic dye solutions employed.

Dye	Solvent	Wavelength range (Å)
Diphenylstilbene	p-Dioxane	3980–4140
Diphenylstilbene	Toluene	4020–4180
popop	Toluene	4100–4280
Dimethyl-popop	Toluene	4220–4420
7-Diethylamino-4-methylcoumarin	Ethanol	4370–4750

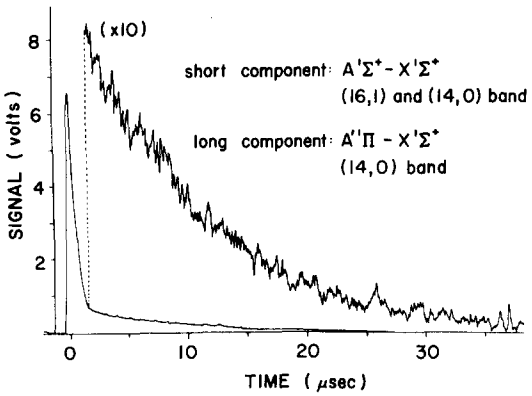

FIG. 3. Fluorescence signal as a function of time using excitation at 4364 Å.

±1 Å. Since the dye laser scan mechanism consists of a sine drive (Molectron DL-300) coupled to a clock motor (Halstrup Model 120-D) the linearity of the wavelength scan is expected to be better than one part in one hundred. This linearity was confirmed by calibrating the dye laser at two extremes of the dye wavelength range using the Hg lamp. The combination of spectrometer calibration and scan nonlinearity results in an error in the wavelength of ±2.0 Å.

For measurements of the rotational line positions of the A'–X bands, better calibration is necessary. In this case the dye laser output is calibrated directly against standard lines from a Hg or Ne lamp in the following manner. Using the 1 m spectrometer in second order with slit widths of 10 μ or less (resulting in a resolution of 0.1 Å), the spectrometer is tuned to the maximum of a standard line. Then the dye laser output, observed through the monochromator, is scanned in wavelength until its transmission is maximized. The wavelength reading, provided by the Molectron DL-300 readout, corresponding to the wavelength of the standard line is then noted. The calibration is repeated using a different standard line and thus a different wavelength output of the same dye. Intermediate dye laser wavelengths are obtained by linear interpolation. Linear extrapolation is also used for wavelengths outside the region spanned by the standard lines. The rotational spectrum of the A'–X bands within the range of that dye is then recorded without altering any of the dye laser components. While scanning the dye laser, an event marker on the recorder indicates the dye laser wavelength readout at regular intervals. The constancy of the distance between these marks is checked to confirm the linearity of the stripchart recorder drive. This results in absolute wavelength accuracy for each line of ±0.2 Å and relative accuracy of ±0.05 Å. Because the dye laser bandwidth is 0.2 Å, no additional effort was made to improve the absolute calibration.

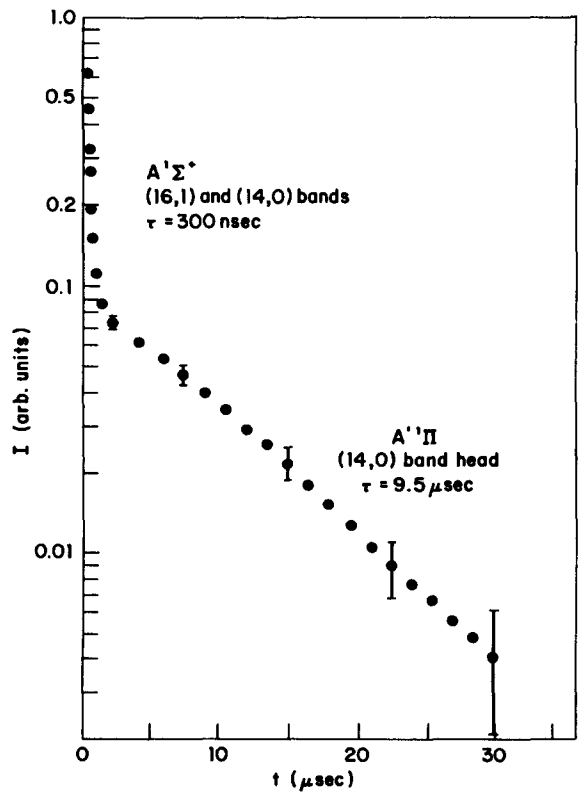

FIG. 4. Plot of the logarithm of the fluorescence signal, given in Fig. 3, as a function of time.

TABLE II. Experimental radiative lifetimes determined for various levels of the BaO $A'\,^1\Pi$ state.

Vibrational band	Rotational lines excited	Radiative lifetime (μsec)
(13,0)	$R(1)$–$R(5)$	8.8
(13,0)	$P(28)$, $Q(30)$, $R(32)$[a]	10
(14,0)	$R(1)$–$R(5)$	9.5
(14,0)	$P(43)$, $Q(45)$, $R(47)$[a]	8.2
(16,0)	$R(1)$–$R(5)$	10
(17,0)	$R(1)$–$R(5)$	9.7

[a]The actual value of J' is uncertain by ±2 units.

III. RESULTS

A. The $A'\,^1\Pi$ radiative lifetime

Figure 3 shows a typical fluorescence decay curve obtained in our experiments. As can be seen, the beginning of the curve represents a combination of laser light, unavoidably scattered into the phototube by the apparatus, and short lifetime fluorescence from a $A\,^1\Sigma^+$–$X\,^1\Sigma^+$ transition, probably resulting from the (16, 1) and (14, 0) bands. Fluorescence from these bands dies away in a few μsec, however, and fluorescence from a long-lifetime state [the $A'\,^1\Pi$–$X\,^1\Sigma^+$ (14, 0) band] may be followed to several $1/e$ points. Figure 4 shows a logarithmic plot of the same decay curve. A double exponential is apparent, caused by the fluorescence from the simultaneously excited A and A' states whose excitation frequencies are within the dye laser bandwidth (0.2 Å). Figures 3 and 4 illustrate in a striking manner how it is possible, using gated detection, to separate the fluorescence of the A' state from that of the A state.

Table II lists the lifetimes of the $A'\,^1\Pi$ state measured at several A'–X bandheads and at individual rotational lines. There appears to be no significant v' or J' dependence of the lifetime over the range of v' and J' investigated. In no case to date have we been able to detect any

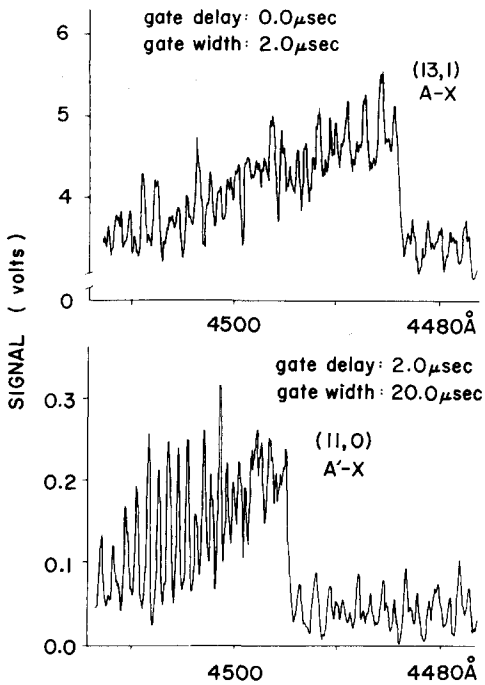

FIG. 5. Lifetime-separated spectrum of the $A'-X$ (11, 0) band showing the discrimination against the stronger $A-X$ (13, 1) band with delayed observation. Note from the signal scales that the $A'-X$ signal is more than an order of magnitude smaller than the overlapping $A-X$ signal.

longer lifetime states in attempts to observe the $a\,^3\Pi$ state. The radiative lifetime of the $A'\,^1\Pi$ state is found to be

$$\tau(A'\,^1\Pi) = 9 \pm 1 \ \mu\text{sec} \ . \tag{2}$$

The 10% uncertainty in τ is primarily a consequence of the statistical noise in the small number of photons collected by the 200 nsec wide gate in 80 laser shots (typically 100 photons). Although it is possible to refine these lifetime measurements, we chose to concentrate our efforts instead on the spectroscopy of the $A'\,^1\Pi$ state.

B. Lifetime-separated spectrum of the BaO A'-X band system

Using the delayed gating technique described in Section II, we have separated the fluorescence of the $A'-X$ band system from the $A-X$ band system in the wavelength range 4000 Å to 4750 Å. Figure 5 illustrates the separation obtained between the (11, 0) bandhead of the $A'-X$ system and the (13, 1) bandhead of the $A-X$ system. In a similar manner we have observed the $(v', 0)$ progression of the $A'-X$ system for $9 \leq v' \leq 18$. We have also observed a few members of the weaker $(v', 1)$ progression, namely, the (10, 1) and (13, 1) bands. The vibrational numbering we use is based on the assignments of Field and agrees with the vibrational numbering adopted by Hsu *et al.*[14] Recently, Wyss and Broida[19] have confirmed this vibrational numbering by isotope studies using ^{18}O. Table III lists the bands observed and the positions of their bandheads. These data are combined with the bandhead positions of Hsu *et al.* to determine the band origin ν_{00} and the vibrational constants ω_0 and $\omega_0 x_0$ of the $A'\,^1\Pi$ state. A least squares fit is used in which their bandhead positions are weighted by a factor of 4 to reflect the fact that the estimated error of their measurements is half that of ours. We find

$$\begin{aligned} \nu_{00} &= 17573 \pm 10 \ \text{cm}^{-1} \ , \\ \omega_0 &= 442.38 \pm 1.1 \ \text{cm}^{-1} \ , \\ \omega_0 x_0 &= 1.693 \pm 0.025 \ \text{cm}^{-1} \ , \end{aligned} \tag{3}$$

where the errors represent one standard deviation. A least squares fit using our data alone results in similar constants within experimental error. In the more customary notation we find $\omega_e = 444.07 \pm 1.1$ cm^{-1} and $\omega_e x_e = 1.693 \pm 0.025$ cm^{-1}, where we have set $\omega_0 y_0$ and higher order terms equal to zero. These values agree fairly well with Field's results[6] of $\omega_e = 448.3 \pm 0.7$ cm^{-1} and $\omega_e x_e = 2.39 \pm 0.13$ cm^{-1}. They are also in very close agreement with the results of Hsu *et al.*,[14] namely $\nu_{00} = 17569 \pm 15$ cm^{-1}, $\omega_0 = 442.8 \pm 1.1$ cm^{-1}, and $\omega_0 x_0 = 1.71 \pm 0.01$ cm^{-1}.

C. Rotational analysis of selected BaO A'-X bands

The rotational structure of a $^1\Pi - ^1\Sigma$ electronic transition consists of P, Q, and R branches whose line positions satisfy the equations[20]

$$\nu = \nu_0 + (B'_v + B''_v)\, m + (B'_v - B''_v - D'_v + D''_v)\, m^2 - 2(D'_v + D''_v)\, m^3 - (D'_v - D''_v)\, m^4 \tag{4}$$

for the $P(m = -J)$ and $R(m = J+1)$ lines, and

$$\nu = \nu_0 + (B'_v - B''_v)\, J(J+1) - (D'_v + D''_v) J^2 (J+1)^2 \tag{5}$$

for the Q lines. In Eqs. (4) and (5) ν_0 is the band origin, B_v the rotational constant, and D_v its first centrifugal correction for the vibrational level v. Because the P and R lines originate from a different Λ component of the $^1\Pi$ state than the Q lines, the rotational constants found from Eq. (4) may have slightly different values from those in Eq. (5).

A bandhead is formed in either the P or R branch depending on the relative size of B'_v and B''_v, and a second "head" is sometimes formed in the Q branch at low J if B'_v and B''_v are nearly equal. Away from the bandhead,

TABLE III. Observed band head positions (cm^{-1}) of the BaO $A'\,^1\Pi$ state. All positions are uncertain by approximately 12 cm^{-1}

v'	$(v', 0)$	$(v', 1)$
9	21 415.5	
10	21 832.7	21 166.2
11	22 240.7	
12	22 636.3	
13	23 037.5	22 378.6
14	23 434.5	
15	23 842.6	
16	24 216.2	
17	24 600.9	
18	24 992.7	

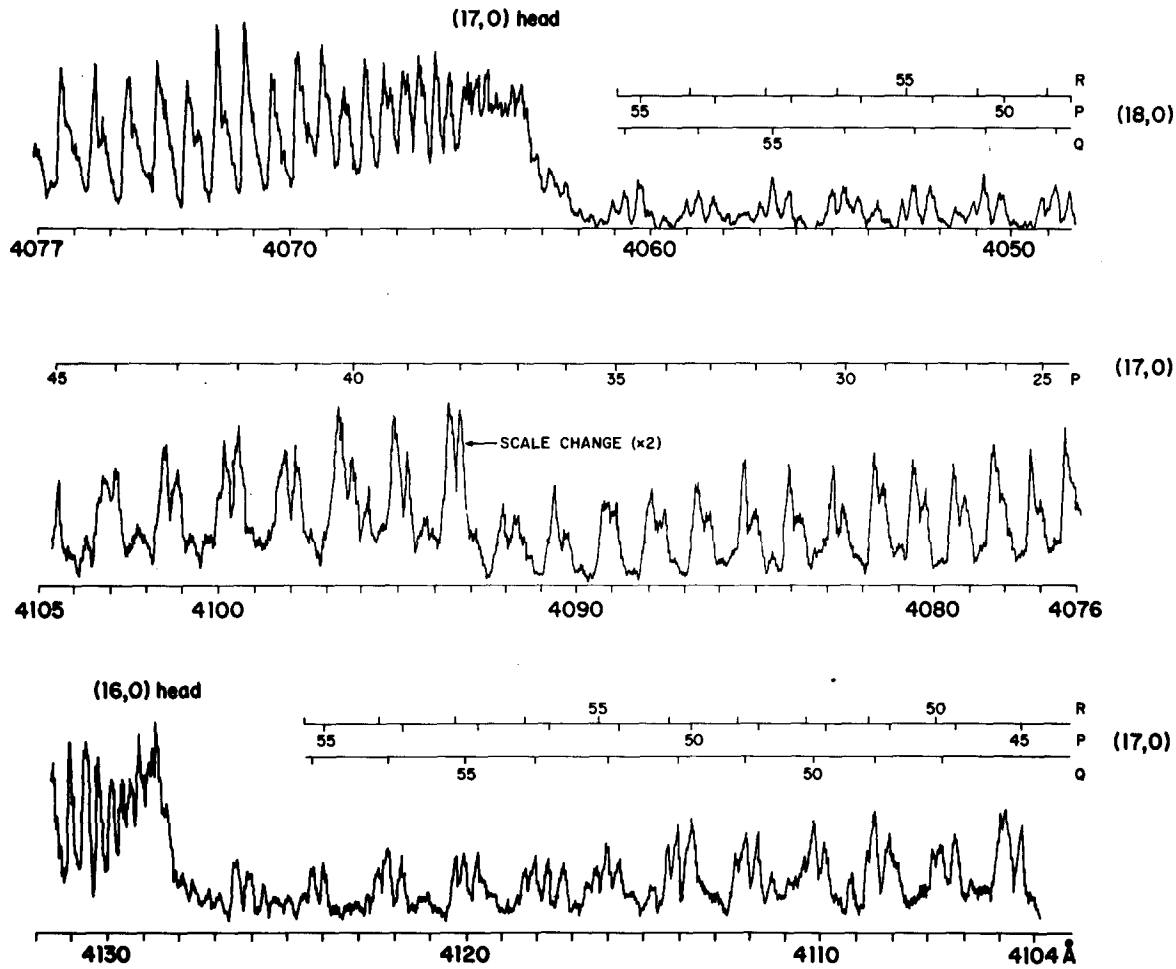

FIG. 6. Lifetime–separated spectrum of the high rotational lines of the (18, 0) band, the (17, 0) band, and the (16, 0) bandhead of the $A'-X$ system. Individual P, Q, and R lines are well resolved for high J transitions.

the P and R lines usually occur in pairs with a separation between the P and R lines which changes only slightly with increasing J. The Q lines usually move in and out of phase with respect to the P and R pairs, because the Q lines follow a different equation. Thus, members of the Q branch can usually be recognized because of the changing phase relationship.[20]

Figures 6 and 7 show the rotational structure of the (17, 0) and (12, 0) bands of the $A'\,{}^1\Pi - X\,{}^1\Sigma^+$ system. At first inspection, it is difficult to recognize that these spectra belong to a ${}^1\Pi - {}^1\Sigma$ transition, because only one head is apparent and no lines exist which show a changing phase relationship to the other lines. The (17, 0) spectrum does show, however, three separate lines at high J, confirming the existence of P, Q, and R branches. Note that for large $(B_v' - B_v'')$ values, the terms in J^2 in both Eqs. (4) and (5) quickly become dominant with increasing J. This results in the formation of a band head at low J in the R branch $(B_v' < B_v'')$, and no formation of a head in the Q branch, in accord with the observed spectra. In addition, the Q lines no longer have a changing phase relationship with the P and R lines, making their identification less obvious. Instead, the lines of all three branches proceed from the head in the form of a trio of lines with slowly changing spacing between adjacent trios, and even more slowly changing relative spacing between the three lines of the set. The appearance of the (17, 0) band is caused by the resolution of the $P(J)$ lines at low J in the three-line set, and the resolution of the $R(J+4)$ and $Q(J+2)$ lines at much higher J values.[21] The appearance of the (12, 0) band as a single line sequence even at high J, is caused by the near coincidence of all three lines of the $P(J)$, $Q(J+2)$, $R(J+4)$ trio, so that the trio appears as one unbroadened line for all lines away from the unresolved area near the band origin $(J \geq 9)$. This trend of slowly changing separation between the lines of the trio for different values of v' precluded complete rotational resolution for all but the high J lines of the (17, 0) and (18, 0) bands. For the (12, 0) band the individual lines are not resolved, but their positions may be accurately measured due to the unbroadened appearance of the signal intensity.

The ground state vibrational and rotational constants of BaO have been well determined by previous spectroscopic studies.[9–11] Because of this, the line positions can be used to determine ν_0 B_v', and D_v' in a least squares manner from Eq. (4) and (5) by fixing B_v'' and D_v'' to their known values.[22] This procedure makes the estimate of the band origin more highly correlated to the estimates of B_v' and D_v' than would be the case if B_v'' and D_v'' were also included as adjustable parameters in the least

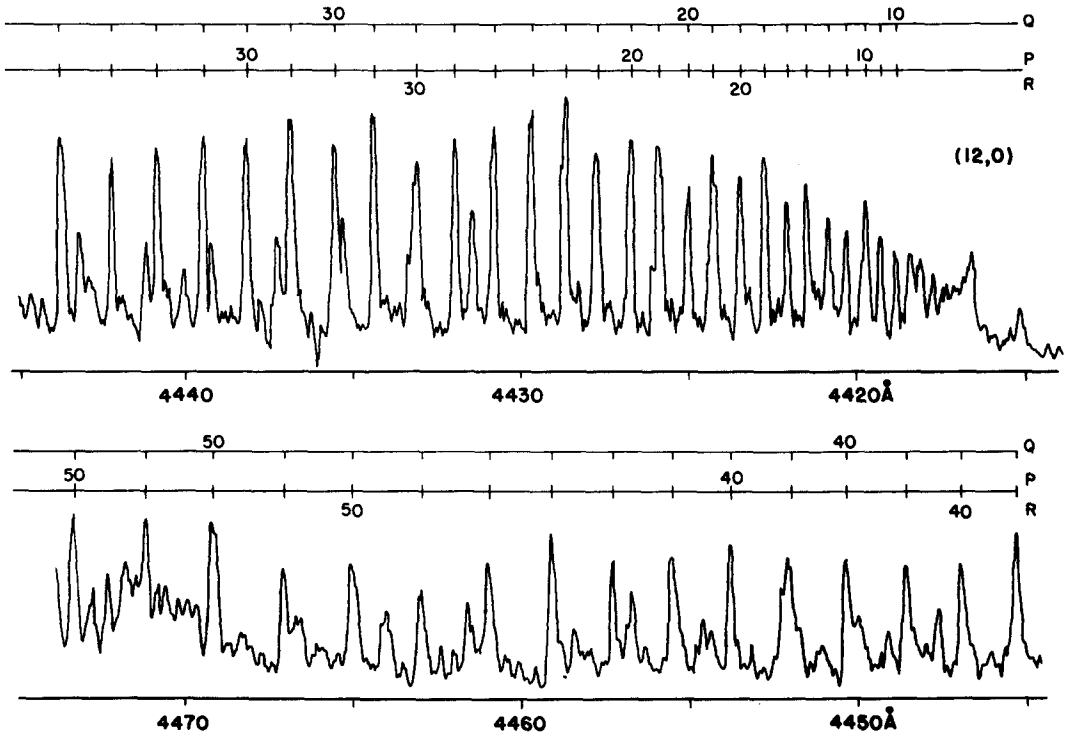

FIG. 7. Lifetime-separated spectrum of the (12, 0) band of the $A'-X$ system. The $P(J)$, $Q(J+2)$, and $R(J+4)$ lines are coincident within the laser bandwidth throughout this spectrum.

squares fit.

Absolute J numbering is obtained by determining the numbering which gives the smallest deviations in the least squares fit. This was unambiguous because the deviations tended to grow rapidly in magnitude for all but the correct numbering. The rotational line assignments of the (12, 0), (17, 0), and (18, 0) bands of the $A'\,^1\Pi-X\,^1\Sigma$ system, their observed vacuum wavenumbers, and the deviations between observed and calculated positions are shown in Table IV. No significant deviations from the predicted line positions are found, as all deviations are within one laser bandwidth.

Since we are fitting lines of high J ($J\sim 50$) we allow for the possibility of Λ doubling in the analysis. This is done by separately fitting the Q lines and the P and R lines to effective B_v values, the difference of which is the Λ doubling constant.[20]

The results of this analysis are given in Table V. For the (12, 0) and (17, 0) bands no significant difference between the two effective B_v values is seen, while for the (18, 0) band, the two differ by more than their combined uncertainties. It is tempting to think we are observing the effect of the Λ doubling constant, but the errors in the B_v values are too large, especially for the Q branch, to encourage us to estimate a value of the Λ doubling constant from the present data.

We have chosen to use the fit to the P, Q, and R lines in the least squares calculation of B_e and α_e. We find

$$B_e' = 0.2235 \pm 0.0016 \text{ cm}^{-1} \,, \qquad (6)$$
$$\alpha_e' = 0.001196 \pm 0.000096 \text{ cm}^{-1} \,.$$

The least squares analysis also provides origins for the (12, 0), (17, 0), and (18, 0) bands, which can be used to calculate ν_{00}, ω_0, $\omega_0 x_0$ by an exact fit. Although the band origin errors are small (see Table V) they do not reflect the absolute wavenumber errors due to the uncertainty in the dye laser wavelength calibration. Consequently, the exact fit is subject to large error. However, if one uses the value of ν_{00} given in Eq. (3), the least squares estimates of ω_0 and $\omega_0 x_0$ from the three band origins agree with the values of ω_0 and $\omega_0 x_0$ given in Eq. (3) to within their error estimates.

IV. DISCUSSION

The application of lifetime-separated spectroscopy to the visible spectrum of BaO demonstrates the power of this method to obtain detailed information about previously inaccessible states, hidden by the presence of stronger transitions in the same spectral region. This technique is not limited to the electronic states of BaO, but is general in nature. In particular, an obvious extension of lifetime-separated spectroscopy would be the investigation of the $A'\,^1\Pi$ states of the other alkaline earth metal oxides.[23,24] In order to extend this technique, the limitations due to lifetime differences, resolution, and calibration must be considered. In the present study, the lifetimes of the $A'\,^1\Pi$ and $A\,^1\Sigma^+$ states of BaO differed by more than an order of magnitude. This permitted their nearly complete separation using simple gating techniques as described in this paper. For two states of more comparable lifetime their separation would require on-line computer analysis of the fluorescence decay curve into its exponential components. The spectroscopic resolution using the laser-induced fluorescence method is limited by the laser bandwidth, and

TABLE IV. Line assignments, their positions (cm^{-1}), and $\nu_{obs} - \nu_{calc}$ (in parentheses) for the (12, 0), (17, 0), and (18, 0) bands of the BaO $A'\ ^1\Pi - X\ ^1\Sigma^+$ band system. Calculated positions are obtained using the constants from the combined P, Q, and R branch analysis of Table V.

	(12, 0)			(17, 0)			(18, 0)		
J	$P(J)$	$Q(J)$	$R(J)$	$P(J)$	$Q(J)$	$R(J)$	$P(J)$	$Q(J)$	$R(J)$
13	22612.32 (−0.29)						24959.01 (0.13)		
14	09.04 (−0.25)						55.39 (0.02)		
15	05.42 (−0.36)	22612.32 (0.29)					51.78 (0.13)		
16	01.79 (−0.26)	09.04 (0.32)					47.98 (0.27)		
17	22598.11 (−0.01)	05.42 (0.21)	22612.32 (−0.39)				43.56 (0.02)		
18	94.18 (0.19)	01.79 (0.30)	09.04 (−0.36)				39.02 (−0.14)		
19	89.73 (0.09)	22598.11 (0.55)	05.42 (−0.48)	24553.88 (−0.04)			34.42 (−0.13)		
20	85.04 (−0.05)	94.18 (0.75)	01.79 (−0.39)	49.05 (−0.10)			29.69 (−0.03)		
21	80.30 (−0.04)	89.73 (0.65)	22598.11 (−0.15)	44.11 (−0.06)			24.72 (0.04)		
22	75.20 (−0.18)	85.04 (0.50)	94.18 (0.05)	39.17 (0.20)			19.50 (0.09)		
23	70.00 (−0.21)	80.30 (0.50)	89.73 (−0.06)	33.81 (0.26)			13.91 (−0.01)		
24	64.60 (−0.24)	75.20 (0.36)	85.04 (−0.21)	27.91 (−0.01)			08.26 (0.05)		
25	58.79 (−0.46)	70.00 (0.33)	80.30 (−0.21)	22.14 (0.07)			02.62 (0.34)		
26	52.99 (−0.48)	64.60 (0.30)	75.20 (−0.35)	16.06 (0.07)			24896.11 (−0.02)		
27	47.19 (−0.29)	58.79 (0.07)	70.00 (−0.39)	09.87 (0.16)			90.09 (0.33)		
28	41.30 (0.01)	52.99 (0.05)	64.60 (−0.42)	02.96 (−0.24)			83.78 (0.60)		
29	35.05 (0.17)	47.19 (0.24)	58.79 (−0.66)	24496.42 (−0.06)			76.53 (0.17)		
30	28.60 (0.33)	41.30 (0.53)	52.99 (−0.68)	89.34 (−0.20)			69.54 (0.20)		
31	21.64 (0.19)	35.05 (0.68)	47.19 (−0.50)	82.14 (−0.24)			62.30 (0.21)		
32	14.70 (0.26)	28.60 (0.83)	41.30 (−0.21)	75.01 (0.00)			54.39 (−0.23)		
33	07.55 (0.33)	21.64 (0.69)	35.05 (−0.06)	67.76 (0.35)			46.73 (−0.21)		
34	22499.65 (−0.14)	14.70 (0.76)	28.60 (0.09)	59.80 (0.20)			38.89 (−0.15)		
35	91.70 (−0.45)	07.55 (0.83)	21.64 (−0.06)	51.48 (−0.09)			30.69 (−0.23)	24844.75 (−0.23)	
36	83.91 (−0.40)	22499.65 (0.35)	14.70 (0.00)	43.47 (0.15)			22.30 (−0.27)	36.67 (−0.37)	
37	75.42 (−0.85)	91.70 (0.03)	07.55 (0.07)	34.93 (0.07)			13.74 (−0.28)	28.40 (−0.48)	24843.95 (−0.20)
38	67.44 (−0.58)	83.91 (0.08)	22499.65 (−0.41)	26.03 (−0.15)			04.99 (−0.24)	19.96 (−0.55)	35.68 (−0.50)
39	59.06 (−0.51)	75.42 (−0.37)	91.70 (−0.73)	17.15 (−0.14)			24796.26 (0.02)	11.58 (−0.33)	27.42 (−0.57)
40	50.99 (0.08)	67.44 (−0.11)	83.91 (−0.69)	08.02 (−0.15)			86.91 (−0.12)	02.66 (−0.45)	19.16 (−0.42)
41	42.62 (0.58)	59.06 (−0.04)	75.42 (−1.15)	24398.67 (−0.17)			77.88 (0.28)	24793.80 (−0.27)	10.54 (−0.41)
42	33.10 (0.13)	50.99 (0.54)	67.44 (−0.89)	88.97 (−0.32)			68.37 (0.42)	84.64 (−0.19)	01.73 (−0.37)
43	24.00 (0.29)	42.62 (1.03)	59.06 (−0.82)	79.69 (0.17)	24396.71 (−0.19)		58.43 (0.34)	75.43 (0.06)	24792.32 (−0.72)
44	14.29 (0.06)	33.10 (0.58)	50.99 (−0.25)	69.77 (0.23)	87.19 (−0.13)		48.69 (0.68)	65.98 (0.29)	83.47 (−0.29)
45	04.60 (0.05)	24.00 (0.74)	42.62 (0.24)	59.44 (0.10)	77.55 (0.04)	24395.64 (−0.45)	37.91 (0.20)	56.10 (0.32)	73.89 (−0.37)
46	22394.56 (−0.11)	14.29 (0.50)	33.10 (−0.22)	49.17 (0.25)	67.69 (0.20)	86.17 (−0.29)	27.51 (0.31)	46.05 (0.38)	64.38 (−0.17)
47	84.38 (−0.20)	04.60 (0.48)	24.00 (−0.07)	38.27 (−0.02)	57.30 (0.04)	76.48 (−0.15)	16.69 (0.22)	35.70 (0.36)	54.63 (0.01)
48	74.31 (0.02)	22394.56 (0.32)	14.29 (−0.30)	27.49 (0.06)	47.04 (0.23)	66.62 (0.05)	05.81 (0.30)	25.18 (0.39)	44.40 (−0.08)
49	64.10 (0.31)	84.38 (0.23)	04.60 (−0.33)	16.36 (0.00)	36.13 (−0.00)	56.06 (−0.25)	24694.83 (0.47)	14.49 (0.45)	34.36 (0.24)
50	53.30 (0.20)	74.31 (0.44)	22394.56 (−0.49)	05.01 (−0.06)	25.18 (−0.07)	45.91 (0.10)	83.31 (0.33)	03.37 (0.31)	23.47 (−0.07)
51		64.10 (0.72)	84.38 (−0.60)	24293.55 (−0.02)	13.94 (−0.20)	34.95 (−0.16)	71.73 (0.35)	24692.27 (0.40)	12.90 (0.15)
52		53.30 (0.61)	74.31 (−0.38)	82.17 (0.31)	02.88 (0.07)	23.99 (−0.19)	59.68 (0.10)	80.44 (−0.02)	01.91 (0.17)
53			64.10 (−0.11)	70.32 (0.40)	24291.31 (0.03)	12.34 (−0.70)	47.64 (0.09)	68.93 (0.09)	24690.80 (0.29)
54			53.30 (−0.23)	57.77 (0.01)	79.81 (0.28)	01.64 (−0.04)	35.50 (0.18)	57.07 (0.07)	78.74 (−0.35)
55				45.30 (−0.09)	68.02 (0.47)	24290.01 (−0.09)	23.06 (0.19)	45.15 (0.20)	67.11 (−0.33)
56				32.96 (0.16)	55.71 (0.35)	78.45 (0.14)		32.77 (0.08)	54.88 (−0.69)
57					43.24 (0.29)	66.43 (0.13)		20.39 (0.19)	43.03 (−0.46)
58					30.49 (0.17)	54.07 (−0.01)			31.07 (−0.13)
59						41.60 (−0.03)			18.21 (−0.48)
60						28.26 (−0.70)			

TABLE V. Molecular constants for the BaO $A'\ ^1\Pi$ state obtained from a least squares fit of the rotational line positions.

Lines analyzed band	branch	ν_0 (cm^{-1})	B_v ($10^{-4}\ cm^{-1}$)	D_v ($10^{-7}\ cm^{-1}$)
(12, 0)	$P\&R$	22636.65 ± 0.12	2084.7 ± 1.9	1.52 ± 0.6
(12, 0)	Q	22637.32 ± 0.17	2083.1 ± 2.9	0.78 ± 1.0
(12, 0)	$P, Q\&R$[a]	22636.84 ± 0.13	2084.9 ± 2.2	1.54 ± 0.7
(17, 0)	$P\&R$	24603.03 ± 0.11	2029.4 ± 1.4	2.60 ± 0.3
(17, 0)	Q	24602.71 ± 1.4	2029.7 ± 11	2.05 ± 2.0
(17, 0)	$P, Q\&R$[a]	24603.04 ± 0.11	2029.0 ± 1.2	2.39 ± 0.3
(18, 0)	$P\&R$	24984.29 ± 0.11	2011.3 ± 1.5	0.83 ± 0.40
(18, 0)	Q	24981.23 ± 0.55	2036.6 ± 5.0	5.54 ± 1.1
(18, 0)	$P, Q\&R$[a]	24984.27 ± 0.11	2010.9 ± 1.4	0.58 ± 0.40

[a]Used in the calculation of B_e and α_e and in calculating line positions used to obtain $\nu_{obs} - \nu_{calc}$ in Table IV.

the wavelength calibration is limited by the availability of standard lines and the linearity of the laser wavelength scan between them. In this study, the rotational spectrum of the BaO A'–X system was obtained with only moderate resolution and precision. However, high resolution studies are possible using intracavity etalons to narrow the laser bandwidth, and using an external Fabrey–Perot interferometer to provide absolute wavelength measurements.

Figure 1 shows that the $a\ ^3\Pi$ and $A'\ ^1\Pi$ states lie close together over a large range of internuclear distances. Although the $a\ ^3\Pi$–$X\ ^1\Sigma^+$ transition is normally forbidden, the mutual interaction between the $a\ ^3\Pi$ and $A'\ ^1\Pi$ states give the former $^1\Pi$ character, making the a–X transition allowed. This suggests the possibility of observing the $a\ ^3\Pi$ state. A search was made for the a–X band system, but we failed to find any feature attributable to the $a\ ^3\Pi$ state. At first this may seem surprising, because the $a\ ^3\Pi$ and $A'\ ^1\Pi$ states are known to interact with each other, causing the large asymmetry in the F_1, F_2, and F_3 components of the $a\ ^3\Pi$ state (the F_2 component is shifted about 48 cm^{-1} compared to the center of gravity of the spin–orbit components).[8] From the observed asymmetry we can estimate that the F_2 component has approximately 25% $^1\Pi$ character while the other components have almost pure $^3\Pi$ character. This implies that the excitation probability of this F component of the $^3\Pi$ state is $\frac{1}{4}$ that of the "pure" $^1\Pi$ state; furthermore, the emission probability per unit time interval is again reduced by $\frac{1}{4}$ compared to the "pure" $^1\Pi$ state. This would result in a $a\ ^3\Pi$ fluorescence signal of $\frac{1}{16}$ that of a "pure" $^1\Pi$ state, and $\frac{1}{4}$ that of the "mixed" $^1\Pi$ state. With our signal-to-noise ratio of approximately 10:1, the failure to detect the a–X band system is not contradictory to the presence of the $a\ ^3\Pi$ state.

Before this work, the only values for the rotational constants of the BaO $A'\ ^1\Pi$ state were those obtained by Field[8] from the analysis of the states which perturb the $A\ ^1\Sigma^+$–$X\ ^1\Sigma^+$ band system. Of the 14 perturbations observed by Lagerqvist, Lind, and Barrow,[11] Field assigned only three as due to the $A'\ ^1\Pi$ state, and the remainder as due to the $a\ ^3\Pi$ state. Consequently, Field could not make an independent analysis of the rotational and vibrational constants of the $A'\ ^1\Pi$ state. Instead, he assumed that the A' and a states had different ν_{00} values but the *same* vibrational and rotational constants. With this assumption he found $\nu_{00} = 17568\ cm^{-1}$, $\omega_0 = 443.9\ cm^{-1}$, $\omega_0 x_0 = 2.39\ cm^{-1}$, $B_e = 0.2244\ cm^{-1}$, and $\alpha_e = 0.0014\ cm^{-1}$. Consequently, it is not surprising that our vibrational and rotational constants differ from those of Field, since his constants were derived from data primarily on the $a\ ^3\Pi$ state. What is surprising is that our results agree so remakably well with those of Field, and therefore confirm the validity of his assumption that the A' and a state potential curves are identical in shape, at least at low vibrational levels of the A' and a states. However, we note that this assumption must fail at higher vibrational levels because these states dissociate to different states of the separated atoms.

Kinetic models of the Ba + oxidant reactions at torr pressures[5–7] have assumed that the $A'\ ^1\Pi$ state has a radiative lifetime of 10 μsec, based on Johnson's[16] observation of some electronic state of BaO having this radiative lifetime. The present determination of the BaO $A'\ ^1\Pi$ state radiative lifetime to be 9 ± 1 μsec strongly suggests that Johnson was observing fluorescence from the A' state and confirms this aspect of the kinetic models.

At low pressures, the $Ba + N_2O$ reaction and the $Ba + O_3$ reaction are known to produce a complex, many-line chemiluminescence spectrum[4] which has been found by Hsu, Krugh, and Palmer[6] to be collisionally unrelaxed at pressures as high as 80 mtorr. At these pressures the time between hard-sphere collisions is 4 μsec, while the time between rotationally inelastic collisions should be much less due to the long-range forces involved. At 80 mtorr, any A' state molecules formed in the reaction should then undergo many rotationally inelastic collisions before radiating because of the long radiative lifetime of the A' state, and would therefore appear collisionally relaxed. Indeed, in our experience with rotational relaxation of reaction products,[17,18] we find that relaxation is evident at pressures as low as 0.1 mtorr when the molecules are subject to collision for a few μsec. We therefore conclude that the many-line emission originates from high vibrational and rotational levels of the short-lived $A\ ^1\Sigma^+$ state. Further support for this conclusion is provided by the observations of Hsu *et al.*[14] that well-formed band heads of the A'–X system occur in the near ultraviolet while on the same photographic plate, the many-line emission spectrum occurs unrelaxed in the blue. Although the lifetime of the $A'\ ^1\Pi$ state is too long to account for the weak many-line spectrum, it is too short to permit this state to be the "dark" precursor to the collision induced A–X spectrum found with high photon yield at pressures of several torr. If the A' state *were* the primary precursor, then the photon yield at low pressure would have to be as large as that at high pressure, in contradiction with experiment, because the primary precursor must be produced with a high yield, and the A' state would radiate before leaving the observation zone. This narrows the choice for the dark precursor to be between the $a\ ^3\Pi$ state, the unobserved $^3\Sigma^+$ state, and high vibrational levels of the ground $X\ ^1\Sigma^+$ state. Although the high photon yields reported for the $Ba + N_2O$ and $Ba + O_3$ reactions refer to A–X emission, the A'–X transition may prove superior as a laser transition for high power

operation since the $A'\ ^1\Pi$ radiative lifetime is more comparable with typical experimentally obtainable chemical pumping rates.

ACKNOWLEDGMENTS

We are very thankful to H. B. Palmer, who stimulated this work by making available to us prior to publication the bandhead positions of the $A'-X$ system obtained in his laboratory. We are also grateful to P. J. Dagdigian, who provided early experimental assistance. This work is supported in part by the U. S. Air Force Office of Scientific Research under grant AFOSR-73-2551A and by the U. S. Office of Naval Research under grant N00014-67-A-0108-0038.

[1]E. Becquerel, Ann. Chim. Phys. **55**, (1859); **57**, 40 (1859); **62**, 5 (1861).

[2]P. Pringsheim, *Fluorescence and Phosphorescence* (Wiley, New York, 1949).

[3]A preliminary report of this work, J. G. Pruett, P. J. Dagdigian, and R. N. Zare, "Observation and Lifetime Measurement of the BaO $A'\ ^1\Pi$ State by Laser Induced Fluorescence," was presented by H. U. Lee at the First Summer Colloquium on Electronic Transition Lasers, at the University of California at Santa Barbara, 17–19 June 1974.

[4]Ch. Ottinger and R. N. Zare, Chem. Phys. Lett. **5**, 243 (1970); C. D. Jonah, R. N. Zare, and Ch. Ottinger, J. Chem. Phys. **56**, 263 (1972); A. Schultz and R. N. Zare, *ibid.* **60**, 5120 (1974).

[5]C. R. Jones and H. P. Broida, J. Chem. Phys. **59**, 6677 (1973); **60**, 4369 (1974); R. W. Field, C. R. Jones, H. P. Broida, *ibid.* **60**, 4377 (1974). C. R. Jones, H. P. Broida, *ibid.* **60**, 4369 (1974).

[6]R. H. Obenauf, C. J. Hsu, H. B. Palmer, J. Chem. Phys. **57**, 5607 (1972); **58**, 2674 (1973); C. J. Hsu, W. D. Krugh, and H. B. Palmer, *ibid.* **60**, 5118 (1974).

[7]D. J. Eckstrom, S. A. Edelstein and S. W. Benson, J. Chem. Phys. **60**, 2930 (1974).

[8]R. W. Field, J. Chem. Phys. **60**, 2400 (1974).

[9]L. Wharton, M. Kaufman and W. Klemperer, J. Chem. Phys. **37**, 621 (1962); L. Wharton and W. Klemperer *ibid.* **38**, 2705 (1963); R. Brooks and M. Kaufman, *ibid.* **43**, 3406 (1965).

[10]P. C. Mahanti, Proc. Phys. Soc. **46**, 51 (1934).

[11]A. Lagerqvist, E. Lind and R. F. Barrow, Proc. Phys. Soc. Lond. A **63**, 1132 (1950).

[12]I. Kovács and A. Lagerqvist, Ark. Fys. **2**, 411 (1951).

[13]R. W. Field, A. D. English, T. Tanaka, D. O. Harris, and D. A. Jennings, J. Chem. Phys. **59**, 2191 (1973).

[14]C. J. Hsu, W. D. Krugh, H. B. Palmer, R. H. Obenauf, and C. F. Aten, J. Mol. Spectrosc. **53**, 273 (1974).

[15]R. N. Zare and D. R. Herschbach, J. Mol. Spectrosc. **15**, 462 (1965).

[16]S. E. Johnson, J. Chem. Phys. **56**, 149 (1972); see also K. Sakurai, S. E. Johnson, and H. P. Broida, J. Chem. Phys. **52**, 1625 (1970).

[17]P. J. Dagidigian, H. W. Cruse, A. Schultz, and R. N. Zare, J. Chem. Phys. **61**, 4450 (1974).

[18]R. N. Zare and P. J. Dagdigian, Science **185**, 739 (1974).

[19]J. Wyss and H. P. Broida (unpublished results). We thank H. P. Broida for communicating this result prior to publication.

[20]G. Herzberg, *Spectra of Diatomic Molecules* (Van Nostrand Reinhold, New York, 1950).

[21]For the range of $B'_v-B''_v$ values applicable here, the $P(J)$, $Q(J+2)$, and $R(J+4)$ lines have nearly the same line positions for all J greater than about $J=9$. This is not true for any other relative J numbering, and hence establishes the relative J numbering. Furthermore, the Q branch line of each trio is identified with the line of highest intensity.

[22]The ground state constants used were the same as those used by T. Wentink, J. Quant. Spectrosc. Radiat. Transfer **12**, 129 (1972), namely, $B''_0 = 0.3119\ \text{cm}^{-1}$ and $D''_0 = 2.65\times10^{-7}\ \text{cm}^{-1}$.

[23]R. W. Field, G. A. Capelle and C. R. Jones, "The $A'\ ^1\Pi-X\ ^1\Sigma$ System of CaO," J. Mol. Spectrosc. 54, 156 (1975).

[24]G. Capelle, H. P. Broida, and R. W. Field, "Photon Yields of $Sr+X$ Reactions ($X=N_2O$, O_3, O_2, NO, Br_2, Cl_2, F_2) and a New SrO $A'\ ^1\Pi-X\ ^1\Sigma$ Band System," J. Chem. Phys. (in preparation).